

# Using *ab initio* calculations in designing bcc Mg–Li alloys for ultra-lightweight applications

W.A. Counts<sup>\*</sup>, M. Friák, D. Raabe, J. Neugebauer

Max-Planck-Institut für Eisenforschung, Max-Planck Str. 1, D-40237 Düsseldorf, Germany

Received 30 April 2008; received in revised form 22 August 2008; accepted 22 August 2008

Available online 1 October 2008

## Abstract

*Ab initio* calculations are becoming increasingly useful to engineers interested in designing new alloys, because these calculations are able to accurately predict basic material properties only knowing the atomic composition of the material. In this paper, single crystal elastic constants of 11 bcc Mg–Li alloys are calculated using density functional theory (DFT) and compared with available experimental data. Based on DFT determined properties, engineering parameters such as the ratio of bulk modulus over shear modulus ( $B/G$ ) and the ratio of Young's modulus over mass density ( $Y/\rho$ ) are calculated. Analysis of  $B/G$  and  $Y/\rho$  shows that bcc Mg–Li alloys with 30–50 at.% Li offer the most potential as lightweight structural material. Compared with fcc Al–Li alloys, bcc Mg–Li alloys have a lower  $B/G$  ratio, but a comparable  $Y/\rho$  ratio. An Ashby map containing  $Y/\rho$  vs  $B/G$  shows that it is not possible to increase both  $Y/\rho$  and  $B/G$  by changing only the composition of a binary alloy.

© 2008 Acta Materialia Inc. Published by Elsevier Ltd. All rights reserved.

**Keywords:** Magnesium alloys; Brittle-to-ductile transition; Density functional; *Ab initio* electron theory; Elastic behavior

## 1. Introduction

Magnesium is a common, lightweight metal that could potentially be more widely used as a structural material in applications where weight saving is crucial. The use of wrought Mg and Mg-alloys is limited in large-scale manufacturing operations for two reasons:

- (1) A lack of room temperature ductility [1]
- (2) The formation of sharp basal or near basal deformation textures (i.e., the tendency of grains to rotate to preferred orientations during deformation) that lead to strong anisotropy in the material [2,3].

In short, Mg and Mg-alloys are difficult to deform at room temperature and, once formed, they have undesirable mechanical properties.

The absence of room temperature ductility and the evolution of strong deformation textures are inherent limitations of the hexagonal close packed (hcp) crystal structure that, to date, have not been completely overcome [4–7]. Changing the crystal structure from hcp to either face centered cubic (fcc) or body centered cubic (bcc) is one way to make Mg more useful. Cubic Mg would be more workable at room temperature, owing to a higher number of available slip systems, and less prone to form disadvantageous deformation textures. These changes would make cubic Mg very attractive from a manufacturing point of view.

The Mg–Li system has a stable bcc phase at room temperature, and the bcc phase is stabilized with as little as 30 at.% Li. Not only does Li stabilize the bcc crystal structure, it also has the advantage of further decreasing the density of the Mg alloy, because Li is the lightest known metal ( $\rho^{\text{Li}} = 0.58 \text{ g cm}^{-3}$ ,  $\rho^{\text{Mg}} = 1.74 \text{ g cm}^{-3}$ ). The resulting Mg–Li alloys are therefore among the lightest possible metallic alloys [8,9].

<sup>\*</sup> Corresponding author.

E-mail address: [w.counts@mpie.de](mailto:w.counts@mpie.de) (W.A. Counts).

In order to investigate the Mg–Li alloy system experimentally, it is necessary first to manufacture the alloys and then determine the relevant mechanical and physical properties. Undertaking such a task is impossible if the necessary infrastructure is not available and, even with the required set-up, casting and then testing Mg–Li alloys will be both time consuming and expensive. A great advantage offered by computational material science tools such as first-principles calculations is the ability to estimate reasonably certain key mechanical and physical properties prior to any experimental work [10–13]. Another advantage offered by first-principles calculations is the ability, with relative ease, to access properties that can be experimentally difficult to determine.

In this paper, *ab initio* calculations are used to provide theoretical guidance in the design of bcc Mg–Li alloys. Single crystal elastic constants are calculated at zero temperature using density functional theory (DFT). These elastic constants are used to calculate Reuss and Voigt bounds and an estimate of homogenized isotropic polycrystalline elastic constants using a self-consistent approach. The homogenized polycrystalline elastic constants are then used to calculate two essential engineering parameters: the bulk modulus/shear modulus ratio (a measure of ductility) and the Young's modulus/mass density ratio (a measure of stiffness per weight). These *ab initio* based results are then used to identify specific alloys that have optimal mechanical properties. Computational results are validated against experimental values taken from the literature. Finally, the properties of Mg–Li alloys are compared with those of Al–Li in order to provide perspective.

## 2. Literature review

There is very little experimental work on the elastic properties of bcc Mg–Li alloys reported in the literature. Trivisonno and Smith [14] measured the single crystal elastic components ( $C_{11}$ ,  $C_{12}$  and  $C_{44}$ ) for four bcc alloys with 0–5 at.% Mg. From these data, they calculated the bulk modulus. Lynch and Edwards [15] experimentally determined the bulk modulus for six bcc alloys between 0 and 70 at.% Mg.

There is also a lack of first-principles work investigating the physical and mechanical properties of bcc MgLi alloys. Hafner [16] derived an optimized first-principles pseudopotential for the binary Mg–Li alloy system. Employing this approach, Hafner predicted the ground state crystal structures, lattice parameters and bulk moduli of 10 Mg–Li alloys (between 0% and 100% Li). Hafner observed good agreement with experiments and predicted lattice parameter values (within 2–3%) and reasonable agreement with bulk moduli (within 25%). However, the equilibrium crystal structure predicted by the pseudopotential did not correctly predict the experimentally observed bcc crystal structure for the alloys with 0–30 at.% Mg.

Hafner and Weber [17] studied the difference between two different bcc structures, B2 (CsCl type) and B32 (NaCl

type), for a single Mg–Li alloy with 50 at.% Li using the LCAO (linear combination of atomic orbitals) method. In this study, they found that the energy of the B2 structure was 115 meV atom<sup>-1</sup> lower than that of B32. Abrikosov et al. [18] used LMTO-ASA-CPA (linear muffin-tin orbitals with Andersen atomic sphere approximation and the coherent potential approximation) to study the effect of Mg concentration dependence on lattice parameter, bulk modulus and Grüneisen constant in bcc Mg–Li alloys, and they observed good agreement with experiments.

While the dependence of mechanical and physical properties, such as lattice parameter and bulk modulus, on alloy composition for bcc Mg–Li alloys has already been investigated, first-principles studies which predict and/or analyze the variations in single crystal and polycrystalline elastic constants ( $Y$  and  $G$ ) as functions of alloy composition are lacking. Polycrystalline elastic constants represent a set of particularly important material properties that engineers must take into account when designing structures. Therefore, identifying trends in these polycrystalline elastic constants can help screen potentially useful bcc Mg–Li alloys.

## 3. Computational approach

### 3.1. *Ab initio* calculations

DFT calculations [19,20] were performed using a plane wave pseudopotential approach as implemented in the Vienna *Ab-initio* Simulation Package (VASP) code [21,22]. Exchange correlation was described by the Perdew–Burke–Ernzerhof generalized gradient approximation (PBE-GGA) [23]. The projector augmented wave (PAW) method [24] was used to describe Mg (taking the Mg 2p and 3s orbitals as valence) and Li (taking the 2s orbital as valence). Convergence checks showed that including the 1s orbital of Li into the valence changes the single crystal elastic constants for bulk Li by less than 2%.

Binary alloys were described by supercells consisting of  $2 \times 2 \times 2$  elementary cubic unit cells with a total of 16 atoms. The plane wave cutoff energy was set to 260 eV, and a  $16 \times 16 \times 16$  Monkhorst–Pack mesh was used to sample the Brillouin zone of the bcc supercells. Fifteen alloy compositions were studied by systematically replacing Mg and Li atoms. Alloy compositions ranged from 6.25 at.% Li to 93.75 at.% Li. For each of the constructed supercells the equilibrium geometry was calculated by minimizing the total energy with respect to atomic positions and supercell shape.

In the present study, only one local atomic arrangement was considered for each composition. These atomic arrangements were chosen in a manner that preserved cubic symmetry. The restriction on a single ordered structure per composition is a severe approximation and can be regarded only as a first step towards modeling and understanding the mechanical properties of Mg–Li alloys at finite temperatures. To estimate the effect of this

approximation, one alloy composition (50 at.% Li) was modeled with two inequivalent ordered structures (B2 and B32). Because the B2 structure is energetically favorable by 19 meV atom<sup>-1</sup> over the B32 structure, the compositional trends in this paper include the B2 structure at 50 at.% Li. The B32 structure is then used as an error estimate.

### 3.2. Calculation and homogenization of elastic constants

Cubic crystals have three independent elastic constants. Consequently, three independent lattice distortions are needed to determine  $C_{11}$ ,  $C_{12}$  and  $C_{44}$ . The first distortion is the isotropic volume change, i.e., the energy–volume dependence from which the bulk modulus  $B_0$  is determined via the Murnaghan equation of state. The second and third distortions are a tetragonal one and a trigonal one (for details, see e.g. Chen et al. [25] and Söderlind et al. [26]). The three distortions lead to three equations from which the single crystal elastic constants can be calculated:

$$B_0 = \frac{(C_{11} + 2C_{12})}{3}; \quad \frac{\partial^2 U^{\text{tet}}}{\partial \delta^2} = \frac{3}{2}(C_{11} - C_{12}); \quad \frac{\partial^2 U^{\text{tri}}}{\partial \delta^2} = 4C_{44} \quad (1)$$

Here,  $\delta$  is strain (or distortion),  $U^{\text{tet}}$  is the strain energy density due to the tetragonal strain, and  $U^{\text{tri}}$  is the strain energy density due to the trigonal strain. Five different tetragonal and five trigonal strains were used to calculate the corresponding elastic constants.

Polycrystalline elastic constants can be estimated from single crystal elastic constants using various homogenization schemes. The upper (or Voigt [27]) bound and the lower (or Reuss [28]) bound on the polycrystalline modulus values are the following:

$$B_R = B_V = B_0; \quad G_R = \frac{5}{4(S_{11} - S_{12}) + 3S_{44}}; \\ G_V = \frac{C_{11} - C_{12} + 3C_{44}}{5} \quad (2)$$

Here,  $B_R$  and  $B_V$  are the Reuss and Voigt bounds on the bulk modulus, and  $G_R$  and  $G_V$  are the Reuss and Voigt bounds on the shear modulus. Additionally, a self-consistent approach can be used to estimate the polycrystalline shear modulus. This type of approach usually gives a better approximation than either Voigt or Reuss. For materials with cubic symmetry, the self-consistent approach simplifies to the following quartic equation [29]:

$$64G_H^4 + 16(4C_{11} + 5C_{12})G_H^3 + [3(C_{11} + 2C_{12})(5C_{11} + 4C_{12}) \\ - 8(7C_{11} - 4C_{12})C_{44}] \cdot G_H^2 - (29C_{11} - 20C_{12})(C_{11} + 2C_{12}) \\ \times C_{44}G_H - 3(C_{11} + 2C_{12})^2(C_{11} - C_{12})C_{44} = 0 \quad (3)$$

Once the homogenized values of  $G$  and  $B$  are known, Young's modulus ( $Y$ ) of a polycrystalline aggregate that is elastically isotropic can be calculated according to

$$Y = \frac{9B_0G}{3B_0 + G} \quad (4)$$

where  $G$  can be  $G_V$ ,  $G_R$  or  $G_H$ .

## 4. Results

### 4.1. Bulk modulus of Mg–Li alloys

The calculated bulk modulus for bcc Mg–Li alloys is compared with experimental values in Fig. 1. The results in Fig. 1 show that bulk modulus varies almost linearly from a minimum at bcc Li ( $B_{\text{Li}} \approx 14$  GPa) to a maximum at bcc Mg ( $B_{\text{Mg}} \approx 35$  GPa). This represents an increase in the bulk modulus of  $\sim 150\%$ . While the simulations do

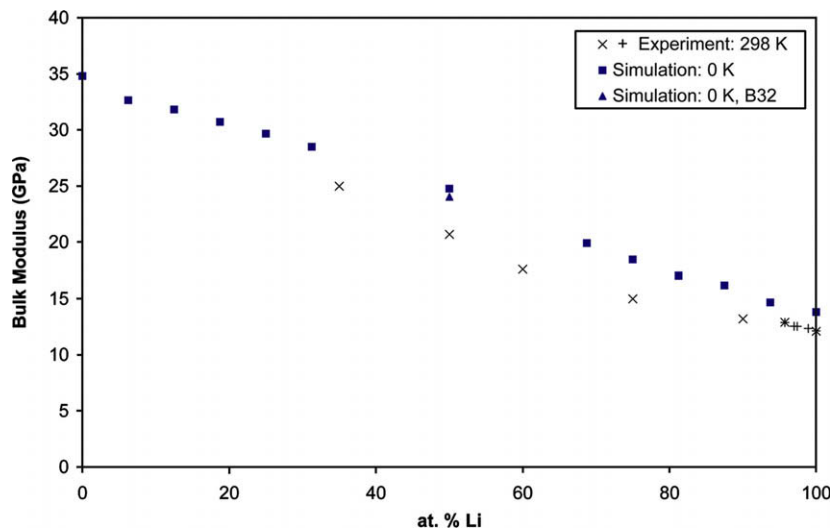


Fig. 1. Simulated and experimental hydrostatic bulk modulus values for bcc Mg–Li alloys. Experimental data: +, Trivisonno and Smith [14]; ×, Lynch and Edwards [15].

capture the correct bulk modulus vs Mg concentration trends, the predicted ground state bulk modulus values are larger than the room temperature experimental values. The difference between the ground state simulation results and the room temperature experiments is between 2 and 5 GPa or between 15% and 20%. The deviations are partly due to the neglect of finite temperature effects and partly due to DFT errors [30]. The effect of local order will be discussed in Section 5.

#### 4.2. Polycrystalline elastic properties of Mg–Li alloys

The polycrystalline shear modulus and Young's modulus were estimated from the DFT predicted single crystal elastic constants using both Voigt and Reuss bounds and a self-consistent based approach. The estimates of the polycrystalline Young's modulus and shear modulus are plotted in Fig. 2.

Fig. 2 shows that changes in  $Y$  and  $G$  as a function of Mg content are highly non-linear. These trends are very different from the almost linear relation found for the bulk modulus, i.e., the other polycrystalline elastic constant (see Fig. 1). The Voigt and Reuss bounds provide maximum and minimum values that the self-consistent homogenization results fall in-between, but not necessarily at the mid-point between the two bounds. For bcc Mg, the self-consistent homogenization scheme is unable to predict elastic constants: all the roots of Eq. (3) are imaginary. This result is in agreement with the Bain path calculations of Jona and Marcus [31], which indicate that bcc Mg is mechanically unstable.

The calculated results in Fig. 2 show that the elastic properties do not change significantly in the range 75–100 at.% Li. The moduli values in this range are quite low ( $Y \approx 12$  GPa and  $G \approx 5$  GPa). As the Mg content

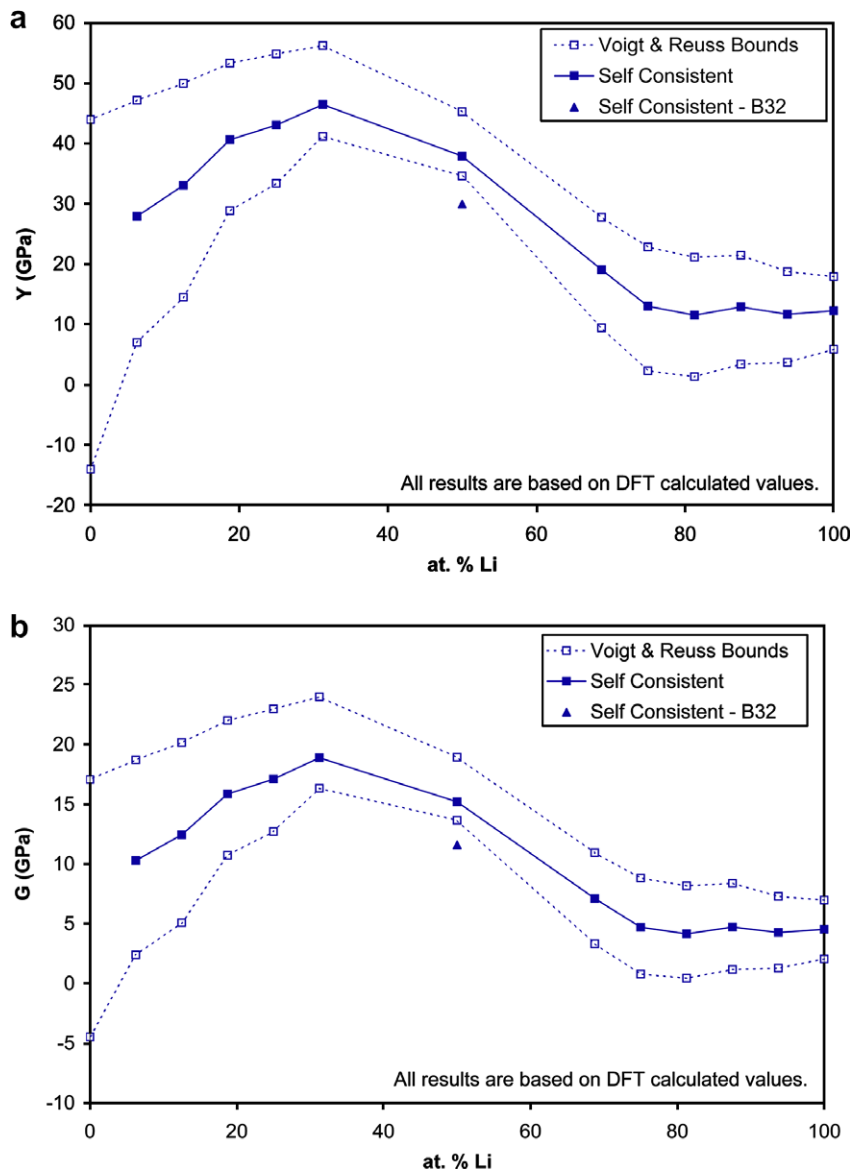


Fig. 2. Isotropic Young's modulus (a) and shear modulus (b) for polycrystalline bcc Mg–Li alloys with a random texture obtained for various homogenization schemes. The results in (a) and (b) are based on the same DFT calculated single crystal elastic constant data.

increases, both the Young's and shear moduli also begin to increase. At  $\approx 30$  at.% Li, both the Young's and shear moduli reach a maximum value ( $Y \approx 46$  GPa and  $G \approx 19$  GPa). Further increase in the Mg content leads to a reduction in both moduli.

### 5. Effect of atomic arrangement: B2 vs B32 at 50 at.% Mg

As discussed in Section 3, the elastic constants for two ordered structures with 50 at.% Li were calculated in order to estimate the effect of local order. As shown in Table 1, the influence of local order on the polycrystalline elastic constants varies. For the isotropic bulk modulus, the effect is small ( $\approx 3\%$ ), while the effect on shear and Young's modulus is more significant ( $\approx 20\%$ ). The importance of these deviations is discussed in Section 6.

### 6. Alloy evaluation and design using *ab initio* derived engineering quantities

To date, there is no known approach by which all the properties of an alloy can be optimized. Instead, improvement in one area (for example stiffness) often comes at the price of a reduced property in another area (such as ductility). Therefore, alloys are designed to fulfill a certain set of prescribed criteria. If bcc Mg–Li alloys are to be used as structural materials for instance in the transportation industry, it must be lightweight (for fuel savings), stiff (for load carrying ability) and reasonably ductile (for sheet forming and crash requirements).

In order to evaluate which alloys will best fulfill the necessary criteria, two separate engineering ratios, which only use DFT calculated quantities, are employed. The first is the ratio between bulk modulus and shear modulus ( $B/G$ ). This ratio has been correlated to the brittle and ductile behavior. The second is the ratio of Young's modulus to density ( $Y/\rho$ ) or specific modulus. This ratio quantifies the stiffness of a material per unit weight.

Throughout this section, the properties of bcc Mg–Li alloys are plotted with those of fcc Al–Li, a commercially available lightweight structural alloy. The polycrystalline Al–Li data ( $B$ ,  $G$ , and  $Y$ ) comes from the DFT data of Taga et al. [32] which was homogenized using the same self-consistent approach (Eq. (3)). Experimental density data for Al–Li alloys were taken from Nobel et al. [33]. In the final section, an Ashby map is constructed by plotting  $B/G$  vs  $Y/\rho$  in order to compare fcc Al–Li and bcc Mg–Li alloys.

Table 1  
Mechanical properties of B2 and B32 bcc Mg–Li alloys;  $G_{\text{Poly}}$  and  $Y_{\text{Poly}}$  are all self-consistent (Hershey) homogenized values

	$B$ (GPa)	$G_{\text{Poly}}$ (GPa)	$Y_{\text{Poly}}$ (GPa)
B2	24.8	15.2	37.9
B32	24.0	11.6	30.0
% Diff.	3.2	23.7	20.8

#### 6.1. Ductility vs brittleness

Knowledge of the polycrystalline elastic constants can also be used with empirical correlations to predict a material's ductility/brittleness. Pugh [34] proposed that the ratio of bulk modulus to shear modulus ( $B/G$ ) could be used to quantify whether a material would fail in a ductile or a brittle manner. Based on the analysis of experimental data for various metals, Pugh proposed that the transition from brittle to ductile behavior occurs around a  $B/G$  value of 1.75. While this critical value does work for many materials, it should not be viewed as a definitive transition point, as the underlying criterion is too simple to capture all the complexity of such a transition, and the transition from brittle to ductile behavior is commonly not sharp.

The  $B/G$  ratio for the polycrystalline bcc Mg–Li alloys is plotted in Fig. 3. The majority of the bcc Mg–Li alloys have a  $B/G$  greater than 1.75, which means in general this alloy system behaves in a ductile manner. For alloys with a high Li content (specifically 70–100 at.% Li), the  $B/G$  ratio is between 2.8 and 4.1, suggesting that these alloys are ductile. Further indication of these alloy's ductility is provided by the fact that both the upper and lower limits are also greater than 1.75. The large  $B/G$  ratio and subsequent ductility of these alloys is a consequence of their relatively small shear modulus ( $G \approx 5$ –7 GPa).

Decreasing the Li content to 30–50 at.% Li results in a significant decrease in the  $B/G$  ratio. This decrease is due to the fact that  $G$  increases faster than  $B$  throughout this composition regime. All the  $B/G$  values in this composition range are below the ductile–brittle transition value, as they range from 1.51 to 1.74. However, the  $B/G$  ratio for the B32 structure is  $\approx 25\%$  greater than that of the B2 structure, illustrating that this ratio is sensitive to the local atomic arrangement. While the low  $B/G$  ratios in this composition regime do indicate brittle behavior, both the upper limit for these alloys and the B32 data point lie above the ductile–brittle transition value, making it difficult to draw a definitive conclusion on the ductility or brittleness of these alloys.

For alloys with less than 30 at.% Li, the  $B/G$  ratio is between 1.9 and 3.2, values that are in the ductile range. However, the bcc alloys in this composition range have no practical value, as the hcp phase is thermodynamically stable at room temperature in this composition range.

#### 6.2. Specific modulus

The specific modulus is an important quantity when comparing lightweight materials for engineering and design purposes. The specific modulus of bcc Mg–Li alloys is plotted in Fig. 4. Bcc Mg–Li alloys with 70–100 at.% Li are both the lightest and least stiff. Consequently, their specific modulus is also on the low end: between 13.9 and 21.6 MPa m<sup>3</sup> kg<sup>−1</sup>. Alloys with less than 20 at.% Li represent the heaviest set of Mg–Li alloys. In this case, their relatively high density results in a specific modulus in the

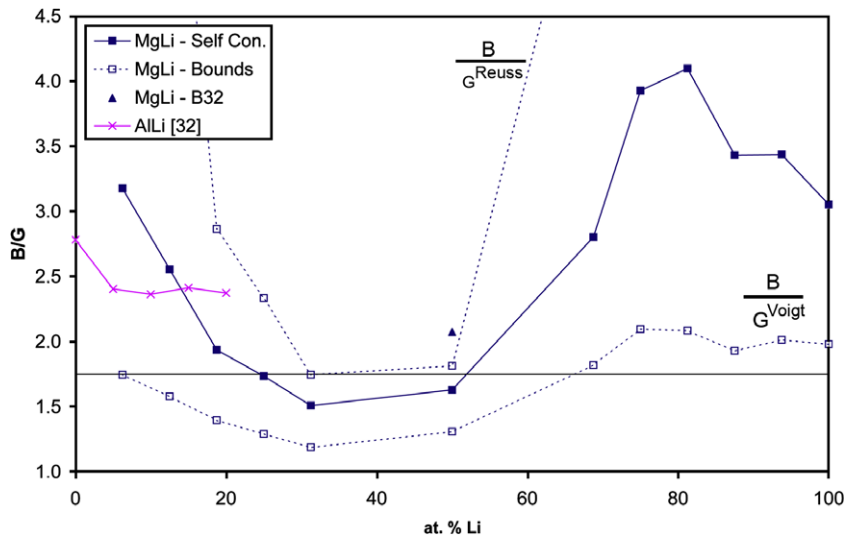


Fig. 3.  $B/G$  ratio for Mg–Li alloys obtained from the Reuss, Voigt and self-consistent homogenization schemes. Al–Li results are based on self-consistent homogenized data. All modulus values are representative of polycrystalline materials with a random texture.

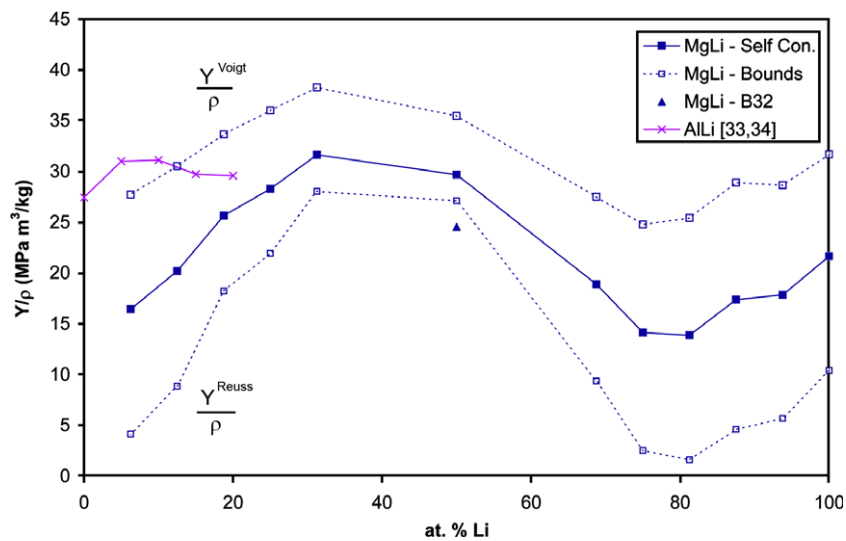


Fig. 4. Specific modulus of Mg–Li and Al–Li. Al–Li results are based on self-consistent homogenized data. Modulus values are representative of polycrystalline materials with a random texture.

range 16.4–25.6  $\text{MPa m}^3 \text{kg}^{-1}$ . Here again, these low Li content alloys are thermodynamically unstable and therefore have no practical value. Mg–Li alloys containing 30–50 at.% Li have the highest values of specific modulus. Their specific modulus ranges between 24.5  $\text{MPa m}^3 \text{kg}^{-1}$  (for B32) and 31.6  $\text{MPa m}^3 \text{kg}^{-1}$  (at 30 at.% Li).

### 6.3. Ashby map of $B/G$ vs specific modulus

A direct comparison between bcc Mg–Li alloys and fcc Al–Li alloys can best be made by plotting  $B/G$  vs specific modulus. The Voigt, Reuss and self-consistent values for Mg–Li alloys with 6–80 at.% Li have been plotted in Fig. 5. The *ab initio* data from Taga et al. [32] for fcc Al–

Li alloys with 5–20 at.% Li are also plotted in Fig. 5. An interesting and unexpected result of this plot is that the Reuss, Voigt and self-consistent values no longer form a lower bound, an upper bound and an approximate average, but virtually coincide on a single (and for this alloy system) universal master curve. Also, the two local structures considered at 50 at.% Li lie on the same line (see inset of Fig. 5). Specifically, the Voigt values define the upper bound on  $Y/\rho$ , the Reuss values define the upper bound on  $B/G$ , and the self-consistent values fall in the region where the Voigt and Reuss values overlap.

The inset graph in Fig. 5 focuses on the self-consistent homogenization part of the master curve. The composition dependence of the self-consistent curve can be explained as

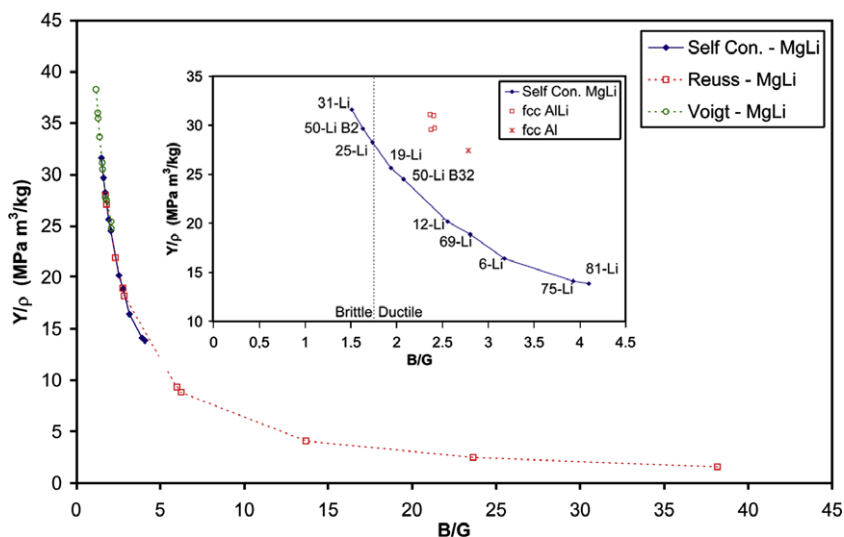


Fig. 5. Ashby map of  $Y/\rho$  vs  $B/G$  for bcc Mg–Li alloys and fcc Al–Li alloys. ( $Y$  = Young's modulus,  $B$  = hydrostatic bulk modulus,  $G$  = shear modulus.) Al–Li results are based on self-consistent homogenized data. All modulus values are representative of polycrystalline materials with a random texture.

follows. The most ductile alloy and least stiff alloy has 81 at.% Li. Decreasing the Li content (75, 69, 50–B32 and 50–B2 at.% Li) results in stiffer less ductile alloys. The stiffest, least ductile alloy has 31 at.% Li. Further decreasing the Li content (25, 19, 12, 6 at.% Li), results in alloys with more ductility and less stiffness.

The universal character of the master curve illustrates an important constraint in alloy design concept: optimization of one property often comes at the expense of another property. For the bcc Mg–Li alloys, it can be seen that an increase in specific modulus is accompanied by a corresponding tendency towards more brittle behavior (i.e., a decrease in the  $B/G$  ratio). The same trend can also be seen in the Al–Li alloys when they are compared with pure fcc Al. For bcc Mg–Li alloys, maximizing  $Y/\rho$  at  $38.3 \text{ MPa m}^3 \text{ kg}^{-1}$  results in a minimum  $B/G$  value of 1.19. The converse is also true: maximizing  $B/G$  at 38 results in a minimum  $Y/\rho$  of  $1.5 \text{ MPa m}^3 \text{ kg}^{-1}$ . An interesting consequence of this analysis is that it does not appear to be possible to increase both  $Y/\rho$  and  $B/G$  by changing only the composition or local order of this binary alloy. The authors expect that the existence of a universal master curve in an Ashby plot will not be restricted to the Mg–Li alloys studied here, but will also be valid for other alloys.

The Ashby map can be used to identify alloys with a combination of properties that are needed in a lightweight structural alloy. Bcc Mg–Li alloys with 30–50 at.% Li are thermodynamically stable (i.e., bcc is the experimentally observed crystal structure at room temperature) and have properties that could potentially rival or better that of Al–Li alloys. However, the predicted  $B/G$  ratio for these Mg–Li alloys is lower than that predicted for Al–Li alloys. Despite the lower  $B/G$  ratio, the increased specific modulus of certain bcc Mg–Li alloys makes this an interesting material system that could offer potential weight savings in the future.

## 7. Conclusions

In order to carry out an *ab initio* guided materials design strategy, ground state DFT calculations were carried out on a systematic set of bcc Mg–Li ordered alloys. The predicted properties of these alloys compare well with available experimental results in the literature. The bulk modulus predictions were within 20% (or 2–5 GPa) and the other polycrystalline elastic constants ( $Y$  and  $G$ ) showed non-linear variations as a function of alloy composition. Alloys with  $\approx 30$  at.% Li were the stiffest, and alloys with greater than 70 at.% Li were the softest.

Using the DFT calculated data, an Ashby map containing  $Y/\rho$  vs  $B/G$  was constructed. Plotting the Reuss, Voigt and self-consistent values of various local arrangements together in this map resulted in a universal master curve. That such a universal curve exists indicates that it is not possible to increase both  $Y/\rho$  and  $B/G$  by changing only the composition or local order of a binary alloy. The Ashby map was used to identify that alloys with 30–50 at.% Li offer the most potential as lightweight structural material. The  $B/G$  ratio for these alloys is close the ductile-to-brittle transition value and less than that of fcc Al–Li alloys. The specific modulus ( $Y/\rho$ ) for these bcc Mg–Li alloys compares favorably with that of fcc Al–Li alloys, indicating that these alloys could offer potential weight savings in the future.

## Acknowledgement

The authors would like to acknowledge funding from the Multi-Scale Modeling of Condensed Matter initiative of the Max Planck Society.

## References

- [1] Agnew SR, Yoo MH, Tome CN. Acta Mater 2001;49:4277.

- [2] Gottstein G. *Physical foundations of materials science*. Berlin: Springer; 2004.
- [3] Philippe MJ, Wagner F, Mellab FE, Esling C, Wegria J. *Acta Metall Mater* 1994;42:239.
- [4] Barnett MR, Nave MD, Bettles CJ. *Mater Sci Eng A* 2004;386:205.
- [5] Nave MD, Barnett MR. *Scripta Mater* 2004;51:881.
- [6] Styczynski A, Hartig C, Bohlen J, Letzig D. *Scripta Mater* 2004;50:943.
- [7] Gehrman R, Frommert MM, Gottstein G. *Mater Sci Eng A* 2005;395:338.
- [8] Jackson RJ, Frost PD. NASA SP-5068; 1967.
- [9] Shen GJ, Duggan BJ. *Metall Trans A* 2007;38:2593.
- [10] Raabe D, Sander B, Friak M, Ma D, Neugebauer J. *Acta Mater* 2007;55:4475.
- [11] Ghosh G, Olson GB. *Acta Mater* 2007;55:3281.
- [12] Ghosh G, Delsante S, Borzone G, Asta M, Ferro R. *Acta Mater* 2006;54:4977.
- [13] Vitos L, Korzhavyi PA, Johansson B. *Phys Rev Lett* 2002;88:155501.
- [14] Trivisonno J, Smith CS. *Acta Metall* 1961;9:1064.
- [15] Lynch RW, Edwards LR. *J Appl Phys* 1970;41:5135.
- [16] Hafner J. *J Phys F Metal Phys* 1976;6:1243.
- [17] Hafner J, Weber W. *Phys Rev B* 1986;33:747.
- [18] Abrikosov IA, Vekilov YH, Korzhavyi PA, Ruban AV, Shilkrot LE. *Solid State Commun* 1992;83:867.
- [19] Hohenberg P, Kohn W. *Phys Rev* 1964;136:B864.
- [20] Kohn W, Sham LJ. *Phys Rev* 1965;140:A1133.
- [21] Kresse G, Hafner J. *Phys Rev B* 1993;47:558.
- [22] Kresse G, Furthmuller J. *Phys Rev B* 1996;54:11169.
- [23] Perdew JP, Burke K, Ernzerhof M. *Phys Rev Lett* 1996;77:3865.
- [24] Blöchl PE. *Phys Rev B* 1994;50:17953.
- [25] Chen K, Zhao LR, Tse JS. *J Appl Phys* 2003;93:2414.
- [26] Söderlind P, Eriksson O, Wills JM, Boring AM. *Phys Rev B* 1993;5844.
- [27] Voigt W. *Lehrbuch der Kristallphysik*. Leipzig: Teubner; 1928.
- [28] Reuss A. *Z Angew Math Mech* 1929;9:49.
- [29] Hershey AV. *J Appl Mech* 1954;21:236.
- [30] Khein A, Singh DJ, Umrigar CJ. *Phys Rev B* 1995;51:4105.
- [31] Jona F, Marcus PM. *J Phys Condens Matter* 2003;15:7727.
- [32] Taga A, Vitos L, Johansson B, Grimvall G. *Phys Rev B* 2005;71:14201.
- [33] Nobel B, Harris SJ, Dinsdale K. *J Mater Sci* 1982;17:461.
- [34] Pugh SF. *Philos Mag* 1954;45:823.